Kopple, K. D., & Go, A. (1977) *J. Am. Chem. Soc. 99*, 7698–7704.
Krauss, E. M., & Chan, S. I. (1982) *J. Am. Chem. Soc. 104*, 6953–6961.
Krishna, N. R., Huang, D. H., Glickson, J. D., Rowan, R., & Walter, R. (1979) *Biophys. J. 26*, 345–366.
Krishna, N. R., Goldstein, S., & Glickson, J. D. (1980) *Biopolymers 19*, 2009–2020.
Krishna, N. R., Huang, D. H., Vaughn, J. B., Heavner, G. S., & Goldstein, G. (1981) *Biochemistry 20*, 3933–3940.
Krishna, N. R., Sarathy, K. P., Huang, D. H., Stephens, R. L., Glickson, J. D., Smith, C. W., & Walter, R. (1982) *J. Am. Chem. Soc. 104*, 5051–5053.
Leichtling, B. J., & Klotz, I. M. (1966) *Biochemistry 5*, 4026–4037.
Lenkinski, R. E., Stephens, R. L., & Krishna, N. R. (1981a) *Biochemistry 20*, 3122–3126.
Lenkinski, R. E., Stephens, R. L., & Krishna, N. R. (1981b) *Biochim. Biophys. Acta 667*, 157–167.
Llinas, M., Klein, M. P., & Nielands, J. B. (1973) *J. Biol. Chem. 248*, 915–923.
Madison, V. (1978) *Biopolymers 17*, 1601–1604.
Molday, R. S., Englander, S. W., & Kallen, R. G. (1972) *Biochemistry 11*, 150–158.
Narutis, V. P. (1983) Ph.D. Thesis, Illinois Institute of Technology, Chicago, IL.
Niccolai, N., Valensin, G., Rossi, C., & Gibbons, W. A. (1982) *J. Am. Chem. Soc. 104*, 1534–1537.
Perrin, C. L., & Johnston, E. R. (1981) *J. Am. Chem. Soc. 103*, 4697–4703.
Philson, S. B., & Bothner-By, A. A. (1979) *Proceedings of the American Peptide Symposium, 6th* (Gross, E., & Meienhofer, J., Eds.) pp 219–222, Pierce Chemical Co., Rockford, IL.
Redfield, A. G. (1978) *Methods Enzymol. 49*, 253–269.
Redfield, A. G., Kunz, S. D., & Ralph, E. K. (1975) *J. Magn. Reson. 19*, 114–117.
Sarathy, K. P., Krishna, N. R., Lenkinski, R. E., Glickson, J. D., Rockway, T. W., Hruby, V. J., & Walter, R. (1981) *Neurohypophyseal Peptide Hormones and Other Biologically Active Peptides* (Schlesinger, D. H., Ed.) pp 211–226, Elsevier/North-Holland, New York.
Walter, R., Smith, C. W., Sarathy, K. P., Pillai, R. P., Krishna, N. R., Lenkinski, R. E., Glickson, J. D., & Hruby, V. J. (1980) *Int. J. Pept. Protein Res. 17*, 56–64.
Woodward, C. K., & Hilton, B. D. (1979) *Annu. Rev. Biophys. Bioeng. 8*, 99–127.

Proton Nuclear Magnetic Resonance Investigation of the Conformation-Dependent Spin Equilibrium in Azide-Ligated Monomeric Insect Hemoglobins†

Gerd N. La Mar,* R. Krishnamoorthi, Kevin M. Smith, Klaus Gersonde, and Hinrich Sick

ABSTRACT: The proton nuclear magnetic resonance spectra of the met–azide complexes of the two allosteric monomeric hemoglobins of the insect larva *Chironomus thummi thummi* have been recorded, assigned, and analyzed. Both the magnitude of the heme methyl shifts and their anomalous temperature dependence indicate a rapid equilibrium between a low-spin ($S = {}^1/_2$) and a high-spin ($S = {}^5/_2$) state. Using the mean methyl hyperfine shift as an indicator of the position of the spin equilibrium, we demonstrate that the axial ligand field is influenced by the heme orientational position in the heme cavity, by the protein conformational state for each heme orientation, and by the presence of a silent point mutation in the heme cavity. The proximal histidyl imidazole exchangeable protons are assigned for the met–azide complexes in both the *Chironomus* hemoglobin and sperm whale myoglobin, and their magnitude reflects a similar percent high-spin component as that derived from the mean heme methyl shift. The pH dependence of the hyperfine shifts reflects a pK consistent with the Bohr effect. The change in percent high spin in the t $\rightleftharpoons$ r transition is found to be too small to account for the Bohr effect. The difference in the position of the equilibrium for the two heme orientations, however, suggests that the two compounds may exhibit different amplitudes of the Bohr effect.

The monomeric hemoglobins from insect larva of *Chironomus thummi thummi* provide ideal subjects for investigating the allosteric control of dioxygen binding. Two of these O_2-binding proteins, labeled CTT III and CTT IV, exhibit marked alkaline Bohr effects in spite of remaining monomeric over the range of pH 5–10, where these proteins are stable in their native form (Sick & Gersonde, 1969; Gersonde et al., 1972, 1976). The Bohr effect is modulated by the particular exogenous ligand bound to the sixth coordination site of the heme iron and is largest for O_2 and considerably smaller for CO (Gersonde et al., 1976; Trittelvitz et al., 1973; Sick & Gersonde, 1974; Steffens et al., 1977). On the other hand, neither the oxidation state of the heme iron (La Mar et al., 1978a) nor the substitution of iron with cobalt (Gersonde et al., 1982) appears to have a significant influence on the Bohr effect. Furthermore, the exchange of proto- for meso- or deuteroporphyrin does not influence the magnitude of the Bohr effect in these hemoglobins (La Mar et al., 1978a; Gersonde et al., 1982). The tertiary structural transition responsible for the Bohr effect is controlled by a single proton, i.e., the formation of a C-terminal salt bridge (Sick et al., 1972; Ribbing & Ruterjans, 1980a), appearing in both the unligated (deoxy) and all ligated states (Trittelvitz et al., 1973; La Mar et al.,

† From the Department of Chemistry, University of California, Davis, Davis, California 95616 (G.N.L., R.K., and K.M.S.), and the Abteilung Physiologische Chemie, Rheinisch-Westfalische Technische Hochschule Aachen, 5100 Aachen, West Germany (K.G. and H.S.). *Received May 31, 1983.* This work was supported by grants from the National Institutes of Health, HL-16087 (G.N.L.) and HL-22252 (K.M.S.), and the Deutsche Forschungsgemeinschaft (K.G.).

0006-2960/83/0422-6239$01.50/0

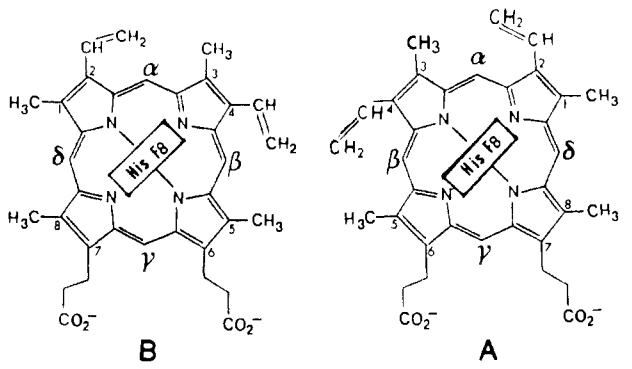

FIGURE 1: Heme orientations: (A) as found in single crystals of Hb III (Steigemann & Weber, 1979); (B) rotated 180° about the α–γ–meso axis from that in (A).

1978a,b, 1981; Sick et al., 1972; Ribbing & Ruterjans, 1980a,b; Krumplemann et al., 1980). The allosteric control of the ligand affinity in hemoglobins is though to occur primarily through changes in the proximal histidyl imidazole–iron bond (Sick et al., 1972; Braunitzer et al., 1974; Shulman et al., 1974; Overkamp et al., 1976; Perutz, 1979, 1980). Since kinetic data on oxygenation reveal that only the ligand off-rate is pH dependent in the monomeric *Chironomus* Hbs[1] (K. Gersonde, unpublished results), the tertiary structural change must influence the axial bond mainly in the ligated form (Gersonde et al., 1982; La Mar et al., 1981). Via induced fit, the exogenous ligand makes the imidazole–iron bond sensitive to the allosteric control by the Bohr proton site. ^{1}H NMR investigations of the nonligated native proteins (La Mar et al., 1981) as well as ESR studies on the Co(II)-substituted insect hemoglobins (Gersonde et al., 1982) find only negligible changes with pH in the iron–histidine bond.

It is noteworthy that ^{1}H NMR studies of both the deoxy- (La Mar et al., 1981) and the metcyano-Hbs (La Mar et al., 1978a, 1980) reveal that, in contrast to the unique structure of CTT III in the crystalline state (Steigemann & Weber, 1979), both Hbs exhibit heme rotational disorder. Thus, these hemoglobins exist in solution as a mixture of two molecular species containing the heme orientation found in the crystal (see A in Figure 1) and that rotated by 180° about the α–γ–meso axis (see B in Figure 1). Since the pK values associated with the Bohr effect differ for the two heme orientations in both the metcyano (La Mar et al., 1978a) and carbonmonoxy forms (Ribbing & Ruterjans, 1980a,b), it is quite possible that the amplitudes of the Bohr-effect curves, i.e., the energies of interaction between ligand and Bohr proton, differ not only between CTT III and CTT IV (Gersonde et al., 1972; Sick & Gersonde, 1974) but also for the two heme orientations of each protein. Lastly, ^{1}H NMR spectra for metcyano-CTT III have shown (La Mar et al., 1983) that splittings of some signals can be resolved for each heme orientation due to a silent mutation in the heme cavity, 57E6(Thr/Ile) (Buse et al., 1979), raising the possibility that this mutation may also influence the iron electronic structure and, hence, the ligand affinity.

Spectroscopic studies on the mixtures of all types of the above-mentioned conformers provide the best current method for assessing potential differences in electronic structure that can influence the function. Detailed information on the electronic structure of heme proteins in solution is particularly readily derived from the ^{1}H NMR spectra of their paramagnetic forms (Wuthrich, 1970; La Mar & Walker, 1978; La Mar, 1979) because the hyperfine shifts exhibited by the attached ligands are sensitive indicators of the imidazole–iron bond (Shulman et al., 1974; Morrow & Gurd, 1975; La Mar et al., 1977, 1981; Nagai et al., 1982). However, changes in protein conformation invariably manifest themselves in both changes in the effective axial field, which would be monitored by the average hyperfine shifts for the four nonequivalent heme methyls (see Figure 1), and changes in the rhombic or in-plane asymmetry, which shows up in variations in the pattern and/or spread of the individual methyl hyperfine shifts (La Mar & Walker, 1973; La Mar, 1979). In order to reach conclusions as to changes in axial field strength, it would be necessary, for example, to monitor all four heme methyl signals.

The ^{1}H NMR spectra of the paramagnetic forms of *Chironomus* Hbs have been studied most extensively in the metcyano forms (La Mar et al., 1978a,b, 1980), where one methyl and one vinyl group exhibited marked shift changes with pH, with relative magnitudes parallel to the known amplitudes of the O_2 Bohr-effect curves. However, a total of only two methyl signals was resolved for each heme disorder component, with the other two obscured by the intense diamagnetic envelope.

An ideal hemoglobin derivative that would likely permit the resolution of the four heme methyl signals and that would provide an amplified probe of the effective axial field under various protein-structural conditions, is the paramagnetic met–azide complex. The azide as an axial ligand in hemoglobins exerts an intermediate ligand field, generally leading to thermal mixture of the high-spin ($S = {}^5/_2$) and low-spin ($S = {}^1/_2$) forms (Scheler et al., 1957; Beetlestone & George, 1964; Gersonde et al., 1970; Iizuka & Kotani, 1974; Morishima & Iizuka, 1974). For the azide derivative of insect hemoglobins, a fraction of about 27% high-spin form at 22 °C has been calculated on the basis of magnetic susceptibility (Scheler et al., 1957; Gersonde et al., 1970). Even small changes in the effective axial field strength would manifest themselves in a shift in the spin-state equilibrium, with stronger fields favoring the low-spin configuration. Since the average heme methyl hyperfine shifts are much larger in all high-spin ferric model complexes and heme proteins than in similar low-spin systems (La Mar & Walker, 1978; La Mar, 1979), a small shift in equilibrium toward the high-spin or low-spin forms will yield significant changes in downfield or upfield shifts.

We report herein on a high-field ^{1}H NMR study of the met–azide complexes of CTT III and CTT IV, which not only confirms that these complexes indeed exhibit the rapid thermal spin equilibrium but also demonstrates that the state of the spin equilibrium is affected by the protein-conformational equilibrium, the heme orientation for a given conformation, and the presence of a silent mutation in the heme pocket. The changes in the position of the spin equilibrium can be directly correlated with the change in the effective axial ligand field strength, which presumably is modulated by either the iron–histidine or iron–azide bonding.

Materials and Methods

Preparation of Hemoglobins. The monomeric hemoglobins III and IV from insect larvae of *Chironomus thummi thummi* were separated from the dimeric components by gel filtration (Sick et al., 1972) and purified by ion-exchange chromatography (Gersonde et al., 1982). A 1-kg mass of frozen larvae (corresponding to about 25 g of hemoglobin) stored for months at −30 °C was shredded at room temperature. The particles

[1] Abbreviations: CTT, *Chironomus thummi thummi*; NMR, nuclear magnetic resonance; ESR, electron spin resonance; DSS, sodium 4,4-dimethyl-4-silapentane-1-sulfonate; Hb, hemoglobin; Mb, myoglobin; Tris, tris(hydroxymethyl)aminomethane.

were suspended in 1 L of 0.1 M phosphate buffer, pH 6.5, saturated to 40% with ammonium sulfate and were homogenized for 5–10 s in a blender, also at room temperature. The following preparative work was performed at 4 °C. The homogenized material was centrifuged for 30 min (Sorvall, type RC-2B, rotor GSA, 12 000 rpm), fat particles were removed from the hemoglobin-containing supernatant, and then the supernatant was dialyzed against concentrated $(NH_4)_2SO_4$ solution, pH 5.8, under continuous stirring. During the dialysis the pH of the salt solution was controlled and readjusted by adding concentrated Na_2HPO_4 solution. The hemoglobin precipitated quantitatively. This precipitate, even when suspended in 300 mL of concentrated $(NH_4)_2SO_4$ solution, pH 5.8, should not be stored for longer than 1 week.

The separation of the monomeric from the dimeric hemoglobin components was performed by gel filtration on Sephadex G-50. A portion of 100 mL of the before-mentioned suspension of the Hb precipitate was centrifuged for 20 min (Sorvall, type RC-2B, rotor GSA, 12 000 rpm). The pellet was dissolved in 150 mL of 0.04 M phosphate buffer, pH 5.5. The resulting Hb solution was dialyzed overnight against 0.04 M phosphate buffer, pH 5.5, and then cleared by ultracentrifugation for 60 min (Sorval, type OTD, rotor T 865, 45 000 rpm). For a complete oxidation of the hemoglobins, hexacyanoferrate was added in a molar ratio of Hb to $K_3Fe(CN)_6$ = 1:2 to the supernatant. A volume of 150–250 mL of met-Hb solution (Hb concentration <1.2 g/100 mL) was then applied to a Sephadex G-50 column (10 × 100 cm) equilibrated with 0.04 M phosphate buffer, pH 5.5. Three fractions, i.e., particle-bound Hb, dimeric components (44%), and monomeric components (27%), were eluted by 0.04 M phosphate buffer, pH 5.5. The collected Hb fractions were dialyzed against concentrated $(NH_4)_2SO_4$ solution, and the Hb precipitate (microcrystals) was stored at 4 °C for years. The monomeric Hb fraction was completely purified from dimeric components by once repeating the gel-filtration procedure as described before.

The separation of the monomeric Hb components CTT I, III, and IV was carried out by ion-exchange chromatography on DEAE-Sephadex A-50. A 3-g amount of the extremely purified monomeric fraction, precipitated in concentrated $(NH_4)_2SO_4$ solution, was dissolved in 300 mL of 0.01 M Tris-HCl buffer, pH 9.0, and was dialyzed against the starting buffer (0.01 M Tris-HCl, pH 9.0). The dialysis was completed when the conductivities of the dialyzate and the starting buffer were practically identical. The monomeric hemoglobins were absorbed on the DEAE-Sephadex A-50 column (6 × 60 cm) equilibrated with the starting buffer. The monomeric hemoglobins I, III, and IV were eluted with a linear gradient of 5 L of 0.01 M Tris buffer, pH 9.0, in 0.15 M NaCl.

The chemical homogeneity of CTT III and IV was checked by polyacrylamide gel (10%) disk electrophoresis at pH 9.5. The R_f values of CTTs III and IV are 0.60 and 0.71, respectively. The Hb components were precipitated in concentrated $(NH_4)_2SO_4$ solution and then redissolved in a small volume of H_2O and dialyzed against H_2O under control of the conductivity of the dialyzate. The lyophilized salt-free hemoglobins were stored at −30 °C. The yields were 24 and 34% for CTT III, and IV, respectively.

Reconstitution of Hemoglobins. The reconstitution of both hemoglobins CTT III and CTT IV with deuterium-labeled hemin was performed as described previously (La Mar et al., 1983).

Preparation of Samples. A typical met-azide sample consisted of dissolving 10 mg of the protein in 0.5 mL of ^2H_2O that was 0.2 M in sodium azide, centrifuging out any precipitate, and adjusting the pH to the desired value with 0.2 M NaO^{2}H or 0.2 M ^{2}HCl. The pH were measured by using an Ingold microcombination electrode and a Beckman 3550 pH meter. The pH readings were not corrected for the isotope effect and are referred to as "pH" whether in pure H_2O or 10% $H_2{}^2O$/90% H_2O. Chemical shifts were referenced to the residual water, which in turn was calibrated against 4,4-dimethyl-4-silapentane-1-sulfonate (DSS).

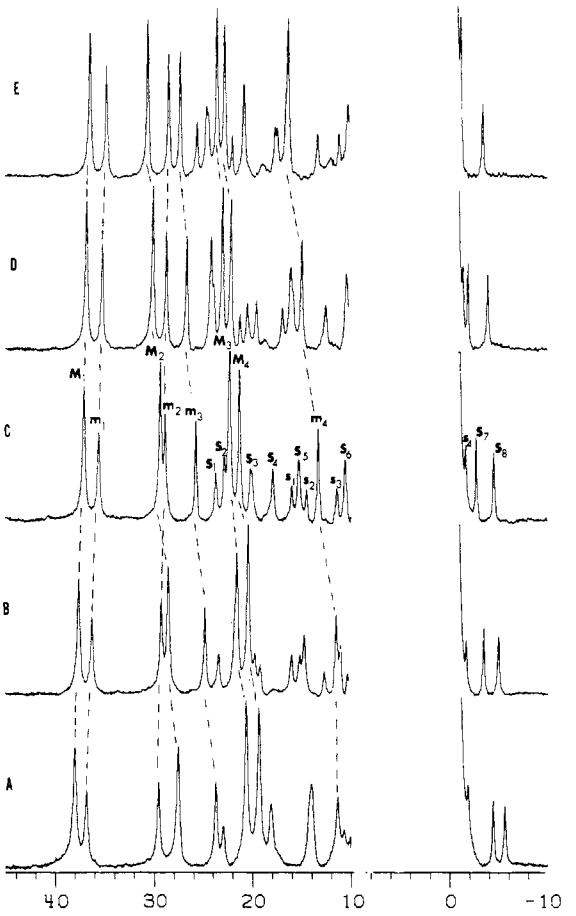

FIGURE 2: 360-MHz ^{1}H NMR spectra of azide–met CTT IV at various temperatures: (A) 5, (B) 15, (C) 25, (D) 35, and (E) 45 °C; "pH" 9.2 in ^2H_2O; shifts are in ppm from DSS. M_1–M_4 represent heme methyls of the major component, whereas m_1–m_4 indicate heme methyls of the minor component. Single-proton intensity peaks are labeled as S_i or s_i depending upon whether they arise from the major or minor component, respectively.

NMR Spectroscopy. ^{1}H NMR spectra were collected on a Nicolet 360-MHz FT machine, operating in the quadrature detection mode. Typically, 5000 transients were collected on a sweep width of 20 kHz with 8K data points and a 12-μs 90° pulse. The residual solvent signal was suppressed with a 150-ms presaturation pulse.

Results

Primary Splitting by Heme Disorder in Hemoglobins III and IV. The hyperfine-shifted regions of the 360-MHz ^{1}H NMR spectra of azide–met CTT IV in ^2H_2O at "pH" 9.2 are illustrated in Figure 2 for several temperatures. The narrow lines with the largest intensity, M_1–M_4 and m_1–m_4, arise from heme methyls. The 3:2 intensity ratio of the two heme orientations, characterized previously for cyanide-ligated and deoxy CTT Hbs (La Mar et al., 1978a, 1980, 1981), establishes that the set M_1–M_4 arises from the major form while m_1–m_4 are due to the four methyls of the minor component. This spectral heterogeneity is due to the primary splitting by

Table I: Heme Methyl Chemical Shifts in Met-Azide CTT Hemoglobins[a]

	Hb III[b] chemical shift, ν (ppm)			Hb IV chemical shift, ν (ppm)		
	pH 6.0	pH 9.5	ΔpH[c]	pH 6.0	pH 9.5	ΔpH[c]
M_1 (8)[d]	37.7	37.5	0.2	38.5	37.2	1.3
M_2 (5)[d]	30.3	29.8	0.5	31.5	29.5	2.0
M_3 (1)[d]	22.5	22.3	0.2	23.5	22.6	0.9
M_4 (3)[d]	21.1	21.1	0.0	22.5	22.0	0.5
ν_M^{obsd} (av)	27.9	27.7	0.2	29.0	27.8	1.2
m_1 (5)[e]	36.5	36.4	0.1	36.3	35.7	0.6
m_2 (1)[e]	29.5	29.7	−0.2	29.0	29.0	0.0
m_3 (8)[e]	27.3	27.0	0.3	27.0	25.9	1.1
m_4 (3)[e]	14.8	14.7	0.1	14.3	13.4	0.9
ν_m^{obsd} (av)	27.0	26.9	0.1	26.7	26.0	0.7
$\nu_M^{obsd} - \nu_m^{obsd}$	0.9	0.8	0.1	2.3	1.8	0.5

[a] Shifts in ppm from DSS at 25 °C. [b] Methyl shifts of the Hb III variant with 57E6(Thr). [c] ΔpH is shift at pH 6.0 minus shift at pH 9.5 (pH-dependent shift change). [d] M_1–M_4 are heme methyls for the major form (methyl assignment in parentheses). [e] m_1–m_4 are heme methyls for the minor form (methyl assignment in parentheses).

the heme disorder. CTT III also shows this primary splitting, although smaller. The methyl shifts for both hemoglobins at 25 °C are listed in Table I.

The remaining single proton resonances are not all completely resolved and are labeled depending on whether their intensity is more consistent with belonging to the major (S_i) or to the minor (s_i) component. While the methyl assignments to the two components are unambiguous (see below), the single-proton assignments are less certain because of the overlap of many of the resonances and, hence, must be considered tentative. The upfield single-proton resonances (shown in Figure 2) are probably vinyl H_β's as found in both low-spin and high-spin systems (La Mar et al., 1978a).

Secondary Splitting in Hb III due to Silent Point Mutation. The spectrum of azide–met-Hb III at 25 °C and "pH" 9.1 is a little more complex, as illustrated by B in Figure 3. The apparent methyls are not as narrow as those in CTT IV, and not all methyl peaks are readily identified. Upon lowering of the temperature to 15 °C (see A in Figure 3), several peaks shift, and all apparent heme methyl signals, M_1–M_4 and m_1–m_4, exhibit a secondary splitting. This complex pattern of individual methyl peaks with areas for three protons requires an assignment by isotope labeling. In C–E of Figure 3, we present for 25 °C the spectra of azide–met CTT III deuterated at positions 1,3, 1,5, and 5,8. These spectra clearly establish that M_2 and m_1 arise from 5-CH_3, M_1 and m_3 are due to 8-CH_3, and M_4 and m_4 originate in 3-CH_3, while 1-CH_3 is responsible for M_3 and m_2. The M_1–M_4 set can be assigned to the major form with the heme orientation as depicted in A of Figure 1, while the m_1–m_4 set arises from the protein with the myoglobin-typical heme orientation as exhibited in B of Figure 1. The splitting of each individual M_i and m_i set is consistent with the intensity ratio of ~1.7 found earlier in the low-spin cyanomet form (La Mar et al., 1983), where the heterogeneity could be directly attributed to a silent point mutation 57E6(Thr/Ile). The methyl shifts of the larger component of the split methyl peak (assigned to the species with Thr at position E6) are included in Table I for each heme orientation.

Influence of pH on Hyperfine Shifts. Plots of the hyperfine shifts at 25 °C vs. "pH" are illustrated in A and B of Figure 4 for azide–met CTT IV and CTT III, respectively. It is

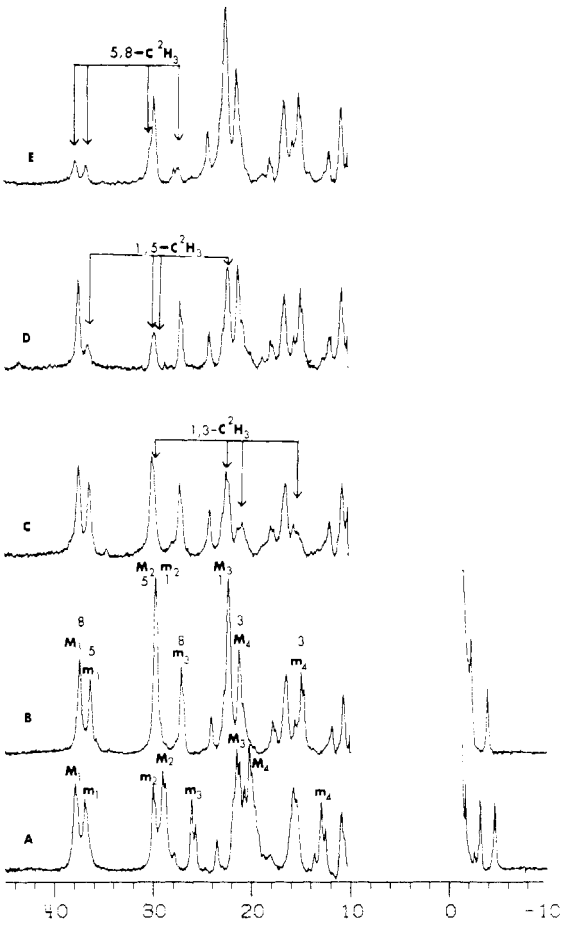

FIGURE 3: 360-MHz ^1H NMR spectra of azide–met CTT III. (A) 15 °C; (B) 25 °C; (C–E) deuterated methyl groups at 1,3-, 1,5-, and 5,8-positions, respectively. Thus, M_1 and m_3 arise from 8-CH_3, M_2 and m_1 from 5-CH_3, M_3 and m_2 from 1-CH_3, and M_4 and m_4 from 3-CH_3. Splitting of the methyl signals due to silent mutation (see text) is better resolved at lower temperature; "pH" 9.1 in ^2H_2O; shifts are in ppm from DSS.

observed that the pH-dependent shift changes are considerably smaller for CTT III than for CTT IV (see also Table I). The data points for M_2 of azide–met CTT IV, which exhibit the largest shift change, fit the Henderson–Hasselbalch equation and yield a pK of 7.7. The inflection points found for other methyl peaks of azide–met CTT IV as well as for azide–met CTT III do not lend themselves well to quantitative determinations of a pK but are consistent with an inflection between pH 7 and 8.

Temperature Dependence of Methyl Proton Hyperfine Shifts. The temperature dependence of the methyl resonances for azide–met CTT IV is displayed in Figure 5 in the form of a Curie plot. Several of the resonances exhibit anti-Curie behavior, which is characteristic of systems undergoing a rapid spin equilibrium (Morishima & Iizuka, 1974; Iizuka & Morishima, 1974; La Mar et al., 1980c). The analogous resonances of azide–met CTT III yield very similar temperature profiles although the poorer resolution makes several peak positions less certain at lower temperatures.

Exchangeable Hyperfine-Shifted Protons. In A and B of Figures 6 we compare the low-field portions of the 360-MHz ^1H NMR spectra of azide–met CTT IV at pH 6.0 in H_2O and ^2H_2O, which clearly reveal one exchangeable peak at 42 ppm that is consistent with arising from the major isomer; a second peak for the other heme-disorder component may exist under M_1.

A similar pair of spectra for azide–met-Mb in H_2O and ^2H_2O are shown in C and D of Figure 6, respectively. Again,

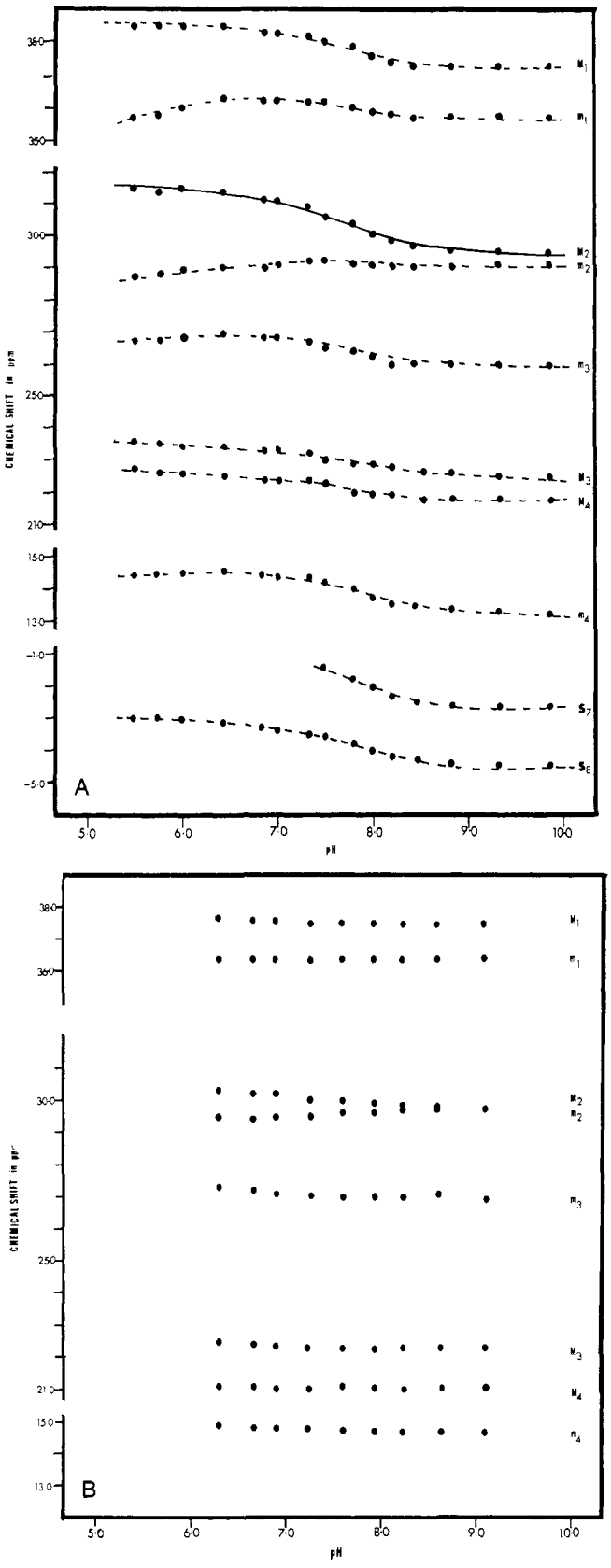

FIGURE 4: pH dependence of hyperfine shifts for azide–met-hemoglobins at 25 °C: (A) CTT IV; (B) CTT III. The solid line drawn through points in (A) represents a computer-fit on the basis of the Henderson–Hasselbalch equation for a single-proton dissociation process, yielding a pK of 7.70 ± 0.05.

a single exchangeable proton peak is observed at 33 ppm. The exchangeable proton shifts for the azide derivatives of Mb and CTT IV, together with the mean methyl resonance shifts of Mb, CTT III, and CTT IV, are compiled in Table II and used

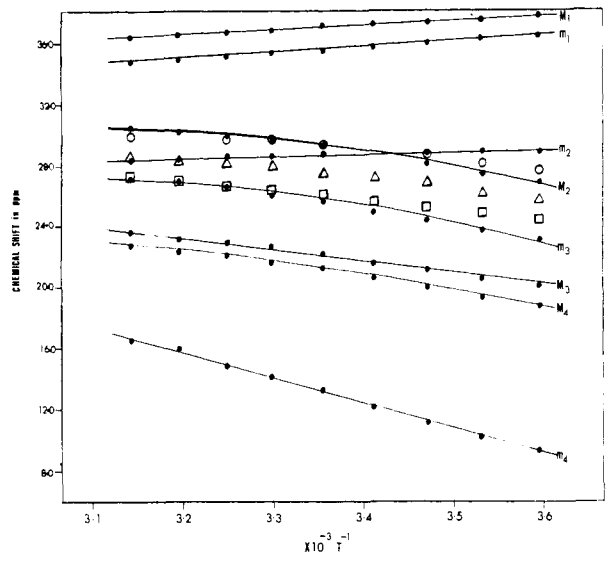

FIGURE 5: Curie plot for methyl resonances of azide–met CTT IV. Also included in the graph are the mean methyl shifts at the corresponding temperature: (O) major component at low pH; (Δ) major component at high pH; (□) minor component at high pH.

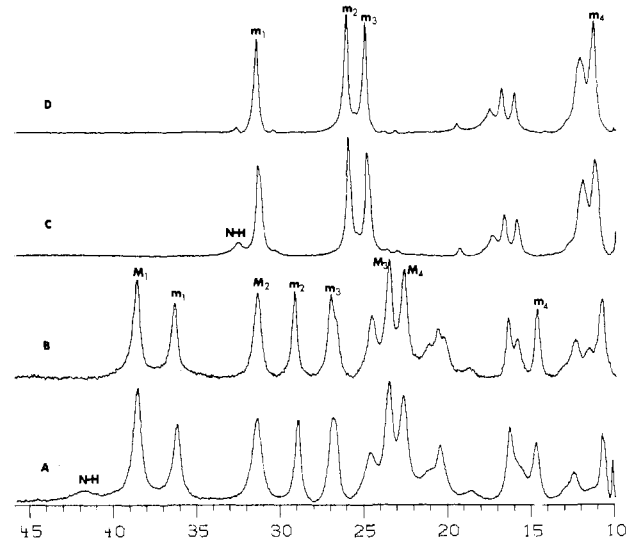

FIGURE 6: Downfield portion of 360-MHz ^{1}H NMR spectra of azide–methemoproteins, "pH" 6.0 at 25 °C; shifts are in ppm from DSS. (A) CTT Hb IV in H_2O; (B) CTT Hb IV in ^2H_2O; (C) sperm whale Mb in H_2O; (D) sperm whale Mb in ^2H_2O. The water-exchangeable proximal histidyl proton is shown for both complexes.

Table II: Determination of Fractional Spin State of Monomeric Met-Azide Hemoglobins

	hemoglobins			
			Hb IV	
	Mb	Hb III	pH 9.5	pH 6.0
ν_M^{obsd} (ppm)[a]	f	28	28	29
HS_M (%)[b]	f	31	31	33
ν_m^{obsd} (ppm)	23[c]	27	26	27
HS_m (%)[d]	18	28	26	28
ν_{NH}^{obsd} (ppm)[e]	33	h	40	42
HS_{NH} (%)[g]	17	h	27	29

[a] Taken from Table I in ppm from DSS; see footnote b in Table I. [b] Calculated from $(\nu_M^{obsd} - \nu_M^{LS})/(\nu_M^{HS} - \nu_M^{LS}) \times 10^2$ for the major component. [c] Data from Figure 6. [d] Calculated from $(\nu_m^{obsd} - \nu_m^{LS})/(\nu_m^{HS} - \nu_m^{LS}) \times 10^2$ for the minor component. [e] In ppm from DSS. [f] Not available (Mb forms practically only the component with heme orientation as in B of Figure 1). [g] Calculated from $(\nu_{NH}^{obsd} - \nu_{NH}^{LS})/(\nu_{NH}^{HS} - \nu_{NH}^{LS}) \times 10^2$. [h] Not resolved.

for determining the fractional spin states in these monomeric hemoglobins.

Discussion

Assignments of Heme Proton Resonances. The two sets of four well-resolved methyl resonances, M_1–M_4 and m_1–m_4, for azide–met CTT IV have the same relative intensities as the two components of the respective cyanomet form (La Mar et al., 1978a, 1980). Therefore, the azide derivative also reflects the two heme orientations depicted in Figure 1, with the more abundant component (M_1–M_4) corresponding to the heme orientation in A. The existence of two distinct heme orientational components on the basis of the rotation around the α–γ-meso axis results in a primary splitting of all methyl resonances.

In the case of azide–met CTT III, a variable secondary splitting of each apparent methyl peak makes assignments to these heme-disorder components based simply on relative intensities much more difficult. However, the results of the isotope labeling at all methyl groups, illustrated in Figure 3, clearly show that both components of the split resonances, M_1–M_4 and m_1–m_4, arise from the heme methyls. The resulting assignments of individual methyl peaks for each heme orientation are given in B of Figure 3. The observation that the azide derivatives of both CTT IV and CTT III have methyl resonances for each heme orientation with essentially the same hyperfine shifts argues strongly that the methyl peaks have the same assignments in both hemoglobins, as previously found for both the cyanomet and deoxy forms (La Mar et al., 1978, 1980a, 1981).

The two components that make up each methyl resonance for azide–met CTT III have approximately the same relative intensities ($\sim$1.7) as found earlier for split methyl peaks in cyanomet CTT III (La Mar et al., 1983), where analysis of the effect of heme substituents in nonsymmetrical and symmetric positions and comparison with cyanomet CTT IV showed that the origin of this secondary heterogeneity was the silent mutation 57E6(Thr/Ile) (Buse et al., 1979). The CTT III variant with Thr in position E6 accounts for the larger component of the split signals and exhibits larger hyperfine shifts for each methyl.

The assignment of the single-proton resonances to the individual heme orientations in met–azide CTT III is precluded due to the secondary heterogeneity; however, such assignments of single-proton resonances in these hemoglobin derivatives are unimportant for the present purposes.

The exchangeable proton peaks in the downfield region of the spectrum (see Figure 6) can be confidently assigned to the proximal histidyl imidazole NH on the basis of the line width and on the fact that the shift is intermediate between that found in high-spin and low-spin ferric hemoglobins (La Mar & de Ropp, 1979; Cutnell et al., 1981). Only one such peak is resolved for met–azide CTT IV and is consistent with arising from the major form in solution. The relative intensities of peaks M_1 and m_1 suggest the possibility that the other exchangeable proton peak, i.e., that of the minor component, is under M_1.

Characterization of Spin Equilibrium. The variable-temperature data in Figure 5 show that none of the methyl resonances obey the Curie law. Some of the methyl peaks (M_1, m_1, and m_2) exhibit chemical shifts that increase only very little with decreasing temperature. Other methyl peaks (m_4 and M_3) are characterized by shifts that go sharply upfield with decreasing temperature. Finally, there are methyl peaks (M_4, m_3, and M_2) that exhibit curvature. Such behavior is characteristic of a system exhibiting an equilibrium between two spin states with very different magnetic moments and with distinct patterns of the hyperfine shifts. The molar magnetic susceptibility of azide–met insect hemoglobin has been found to be 5170×10^6 cgs units at 22 °C, indicating a 27%/73% high/low-spin mixture, whereas the cyanomet complex of Mb is purely low spin with 1630×10^6 cgs units; the fluoride–met complex of insect Hb is purely high spin with $14\,700 \times 10^6$ cgs units (Scheler et al., 1957; Gersonde et al., 1970). Furthermore, NMR data (Morishima & Iizuka, 1974) have been reported for the azide and imidazole complexes of metmyoglobin, where changes in volume magnetic susceptibility were independently monitored. The purely high-spin ($S = {}^5/_2$) state is known to have large average methyl hyperfine shifts ($\bar{\nu}_{Me}^{HS}$ = 50–60 ppm) (La Mar & Walker, 1978; Budd et al., 1979; La Mar, 1979; La Mar et al., 1980c). The low-spin ($S = {}^1/_2$) state yields much smaller mean methyl shifts ($\bar{\nu}_{Me}^{LS}$ = 16 ppm) but usually exhibits a much larger in-plane asymmetry or spread in the individual methyl shifts (La Mar & Walker, 1978; La Mar, 1978).

It is the in-plane assymmetry that largely accounts for the variable deviations from Curie behavior found for individual methyl peaks. Thus M_1 (8-CH_3) and m_1 (5-CH_3) are farthest downfield in low-spin complexes of CTT IV and, hence, have the smallest shift difference between the two spin states; this leads to the smallest deviations from Curie behavior. m_4 (3-CH_3), on the other hand, resonates furthest downfield in the high-spin form but occurs in the diamagnetic envelope in the low-spin form, leading to the observed anti-Curie behavior. Thus, the degree of deviation from Curie behavior for individual methyls can be qualitatively correlated with the expected shift patterns in the two contributing spin states, as also discussed previously for azide–met-Mb (La Mar et al., 1980c).

The appropriate ^{1}H NMR index of the deviation from Curie behavior of the overall magnetic moment of the iron is the observed mean chemical shift of the four heme methyls, $\langle\nu\rangle_{Me}^{obsd}$, which averages out the in-plane asymmetry (La Mar, 1979). The value of this parameter at 25 °C is included in Table I for both hemoglobins and is also plotted for azide–met CTT IV as a function of temperature in Figure 5. Thus, the mean observed methyl shift is given by the relationship:

$$\langle\nu\rangle_{Me}^{obsd} = f^{HS}\bar{\nu}_{Me}^{HS} + f^{LS}\bar{\nu}_{Me}^{LS} \quad (1)$$

where f^{HS} and f^{LS} are the mole fractions of high-spin and low-spin species present in solution. Since $\bar{\nu}_{Me}^{HS}$ is much larger than $\bar{\nu}_{Me}^{LS}$, the temperature dependence found for $\langle\nu\rangle_{Me}^{obsd}$ in Figure 5 dictates that the low-spin state is stabilized at lower temperature.

A semiquantitative estimate of the state of the spin equilibrium can be made as follows: Low-spin ferric hemoglobins and model complexes exhibit $\bar{\nu}_{Me}^{LS} \approx 16$ ppm (La Mar & Walker, 1978; La Mar, 1979), whether the axial ligands are both imidazoles, cyanides, or one of each. Hence, we can assume that the low-spin form of any azide–methemoglobin will have essentially the same $\bar{\nu}_{Me}^{LS}$. Since the fraction of high-spin forms in azide–met-Mb is known to be 20% from magnetic susceptibility measurements (Scheler et al., 1957; Iizuka & Morishima, 1974), we can calculate the value $\bar{\nu}_{Me}^{HS}$ in eq 1. The value 55 ppm agrees well with both an estimate made earlier by analyzing the temperature dependence of individual shifts (Iizuka & Morishima, 1974) and mean shift values observed for purely high-spin forms of metmyoglobin containing N-bound sixth ligands such as NCO and NCS (Budd, 1978). We now make the reasonable assumption that these values of 16 and 55 ppm are valid for the *Chironomus* Hbs as well. As shown in Table II, this leads to an estimate of 31% high-spin fraction for the major component of the azide

derivatives of both insect hemoglobins at alkaline pH.

An independent confirmation of the validity of such a semiquantiative determination of the composition of the spin equilibrium is obtained by applying eq 1 to the observed hyperfine shift for the proximal histidyl imidazole NH peak. Low-spin ferric heme proteins yield a shift for $\bar{\nu}_{NH}^{LS} \approx 20$ ppm (La Mar, 1979; Cutnell et al., 1981), while high-spin forms have so far yielded $\bar{\nu}_{NH}^{HS} \approx 95$ pm (La Mar & de Ropp, 1979; La Mar, 1979). As also shown in Table II, using these values as independent of the hemoglobin chain and $\bar{\nu}_{NH}^{obsd} = 33$ and 42 ppm, we obtain 17 and 27% high-spin character for the azide derivatives of Mb and CTT IV, respectively, which is in reasonably agreement with the values derived from the mean methyl shifts. The fraction of high-spin species in a azide–met inspect hemoglobin has been confirmed earlier by the independently measured magnetic susceptibility (Scheler et al., 1957; Gersonde et al., 1980). The data in Table II indicate that the *Chironomus* Hbs exhibit a significantly larger fraction of high-spin species at 25 °C than myoglobin, which dictates that the effective axial field is weaker in insect Hbs than in myoglobin.

Influence of Protein Conformation on Spin Equilibrium. The influence of pH on the hyperfine-shifted heme methyls is shown in Figure 4; the pH-dependent shift changes are consistent with an equilibrium between two conformation states modulated by a single proton. The pK value determined for M_1 of azide–met CTT IV is consistent with that associated with the Bohr effect (Gersonde et al., 1972; Sick & Gersonde, 1974; Steffens et al., 1977). That we are monitoring the tertiary conformational transition responsible for the Bohr effect is also supported by the larger magnitudes of the shift changes in CTT IV than in CTT III (La Mar et al., 1978a, 1981). NMR studies on deoxy (La Mar et al., 1981), carbonyl (Ribbing et al., 1980a,b), and metcyano (La Mar et al., 1978a,b) forms of these two hemoglobins have all revealed pH changes at the heme consistent with a single pK that can be attributed to the Bohr proton. It thus appears reasonable to assume that the observed single pK in the metHbN$_3$'s is due to the same Bohr proton site.

As shown by the data in Figure 4 and Table II, converting from the high-pH (r) to the low-pH (t) conformation results in an increase in hyperfine shifts for both the proximal histidyl imidazole NH and the mean heme methyl proton hyperfine shifts, and this increase is larger for CTT IV than for CTT III. This is observed for both heme orientations, although the effect is larger in the major form (A in Figure 1). The fact that both the NH and mean methyl hyperfine shifts change in the same direction during the t $\rightleftharpoons$ r transition strongly supports the interpretation that both shift changes arise primarily from a change in position of the spin equilibrium rather than from direct influences of the protein structure on the shifts for one of the two contributing spin states. If influences of the protein would occur primarily in $\bar{\nu}_{Me}^{HS}$ and/or $\bar{\nu}_{Me}^{LS}$, the well documented cis effect (Buchler et al., 1978) would require that the shift changes be in opposite directions. Thus, we can conclude that the high-affinity or high-pH (r) state possesses a stronger axial ligand field than the low-affinity or low-pH (t) state.

Comparison of the mean methyl hyperfine shifts for the two heme orientations for each protein reveals that the shifts are smaller for the minor (m_1–m_4) than for the major (M_1–M_4) components (see Table I). This indicates that the axial field is slightly weaker for that heme orientation that had been found in the X-ray crystal structure, i.e., the major component (A in Figure 1). Therefore, we may assume that the ligand affinity of the major heme-disorder component is smaller than that for the minor component. This assumption is qualitatively confirmed by O_2-binding equilibrium studies on monomeric insect hemoglobins performed under repeated cycles of oxygenation and deoxygenation. When deoxygenation cycles are run, the O_2 affinity increases, accompanied by a relative increase in the minor component. Finally, the O_2 affinity becomes constant when heme interconversion has reached equilibrium (K. Gersonde, unpublished results).

Lastly, it may be noted in A and B of Figure 3 that each methyl peak exhibiting the secondary splitting due to the 57E6(Thr/Ile) mutation has the smaller component on the higher field side. This dictates that the average methyl hyperfine shift also depends on the nature of the amino acid at position E6. Although this point mutation has no influence on the allostery itself, i.e., it does not change the Bohr effect, it modulates the azide binding by modifying the local environment of the ligand, and thus the ligand field of the heme iron and the spin equilibrium are affected.

Inasmuch as the pH-dependent relative mean methyl hyperfine shift changes for met–azide CTTs III and IV are qualitatively consistent with the relative amplitudes of the Bohr-effect curves for these two hemoglobins, one may suggest that the change in bonding of axial ligands (proximal imidazole and azide) responsible for the shift in the spin equilibrium may also, at least in part, control the change in function. The lower fraction of high-spin contribution in the high-affinity (r) form at high pH in both hemoglobins indicates stronger axial bonding than that in the low-affinity (t) conformation at low pH. This is consistent with earlier findings for tetrameric metaquo-Hb, where the low-affinity quaternary T state exhibited a larger high-spin contribution than the high-affinity quaternary R state hemoglobin (Perutz et al., 1974). Thus, our finding indicates allosterically controlled strains on the azide binding, i.e., relaxation of the azide–iron bond in the ligated t state or possibly compression of the azide–iron bond in the ligated r state. Thus allosterically controlled differences in axial bonding must occur wholly within the ligated state since we have shown by several methods (ESR, Mössbauer effect, NMR, on-kinetics of ligand binding) that iron–imidazole bonding is unaffected by the t $\rightleftharpoons$ r transition in the deoxy forms.

If we estimate the standard free energy of the spin-state change from (Perutz et al., 1974)

$$\Delta G_s = -RT \ln (f^{LS}/f^{HS}), \quad (2)$$

we find that the t $\rightleftharpoons$ r transition produces an energy change of only 50–60 cal/mol for azide–met CTT IV. Therefore, this change in axial bonding detected as change in spin equilibrium can make only a minor contribution to the total Bohr-effect interaction energy in CTT IV, which has been determined as 1080 cal/mol for O_2 binding and 480 cal/mol for CO binding (Gersonde et al., 1972; Sick & Gersonde, 1974). However, the sensitivity of the mean methyl shift to pH is larger in the major than in the minor components for each protein, and ΔG_s differs by 140–145 cal/mol for the two heme orientations of azide–met-Hb IV. Thus, the present data suggest that the amplitude of the Bohr-effect curve probably also depends on the orientation of the heme, with a larger Bohr effect for the heme orientation as indicated in A of Figure 1. Planned studies on O_2 binding of monomeric Chironomus Hbs possessing variable ratios of heme orientations may provide more evidence for this hypothesis.

Acknowledgments

We thank Helga Gorgels for her skillful technical assistance.

Registry No. Heme, 14875-96-8.

References

Beetlestone, J., & George, P. (1964) *Biochemistry 3*, 707–714.

Braunitzer, G., Buse, G., & Gersonde, K. (1974) in *Molecular Oxygen in Biology: Topics in Molecular Oxygen Research* (Hayashi, O., Ed.) pp 183–218, North-Holland, Amsterdam.

Buchler, J. W., Kokisch, W., & Smith, P. D. (1978) *Struct. Bonding (Berlin) 34*, 79–134.

Budd, D. L. (1978) Ph.D. Thesis, University of California, Davis.

Budd, D. L., La Mar, G. N., Langry, K. C., Smith, K. M., & Nayyir-Mazhir, R. (1979) *J. Am. Chem. Soc. 101*, 6091–6096.

Buse, G., Steffens, G. J., Braunitzer, G., & Steer, W. (1979) *Hoppe-Seyler's Z. Physiol. Chem. 360*, 89–97.

Cutnell, J. D., La Mar, G. N., & Kong, S. B. (1981) *J. Am. Chem. Soc. 103*, 3567–3572.

Gersonde, K., Sick, H., & Wollmer, A. (1970) *Eur. J. Biochem. 15*, 237–244.

Gersonde, K., Noll, L., Gaud, H. T., & Gill, S. J. (1976) *Eur. J. Biochem. 62*, 577–582.

Gersonde, K., Twilfer, H., & Overkamp, M. (1982) *Biophys. Struct. Mech. 8*, 189–211.

Huber, R., Epp, O., & Formanek, H. (1969) *J. Mol. Biol. 42*, 591–594.

Huber, R., Epp, O., & Formanek, H. (1970) *J. Mol. Biol. 52*, 349–354.

Iizuka, T., & Kotani, M. (1969) *Biochim. Biophys. Acta 181*, 275–286.

Iizuka, T., & Morishima, I. (1974) *Biochim. Biophys. Acta 371*, 1–13.

Krumpelmann, D., Ribbing, W., & Ruterjans, H. (1980) *Eur. J. Biochem. 108*, 103–109.

La Mar, G. N. (1979) in *Biological Applications of Nuclear Magnetic Resonance* (Shulman, R. G., Ed.) pp 305–343, Academic Press, New York.

La Mar, G. N., & Walker, F. A. (1978) in *The Porphyrins* (Dolphin, D., Ed.) Vol. 4, pp 61–157, Academic Press, New York.

La Mar, G. N., & de Ropp, J. S. (1979) *Biochem. Biophys. Res. Commun. 90*, 36–41.

La Mar, G. N., Budd, D. L., & Goff, H. (1977) *Biochem. Biophys. Res. Commun. 77*, 104–110.

La Mar, G. N., Overkamp, M., Sick, H., & Gersonde, K. (1978a) *Biochemistry 17*, 352–361.

La Mar, G. N., Viscio, D. B., Gersonde, K., & Sick, H. (1978b) *Biochemistry 17*, 361–367.

La Mar, G. N., Budd, D. L., Smith, K. M., & Langry, K. C. (1980a) *J. Am. Chem. Soc. 102*, 1822–1827.

La Mar, G. N., Smith, K. M., Gersonde, K., & Overkamp, M. (1980b) *J. Biol. Chem. 255*, 66–70.

La Mar, G. N., Budd, D. L., & Smith, K. M. (1980c) *Biochim. Biophys. Acta 627*, 210–218.

La Mar, G. N., Anderson, R. R., Budd, D. L., Smith, K. M., Langry, K. C., Gersonde, K., & Sick, H. (1981) *Biochemistry 20*, 4429–4436.

La Mar, G. N., Anderson, R. R., Chacko, V. P., & Gersonde, K. (1983) *Eur. J. Biochem.* (in press).

Morishima, I., & Iizuka, T. (1974) *J. Am. Chem. Soc. 96*, 5279–5283.

Morrow, J. S., & Gurd, F. R. N. (1975) *CRC Crit. Rev. Biochem. 3*, 221–287.

Nagai, K., La Mar, G. N., Jue, T., & Bunn, H. F. (1982) *Biochemistry 21*, 842–847.

Overkamp, M., Twilfer, H., & Gersonde, K. (1976) *Z. Naturforsch., C: Biosci. 31C*, 524–533.

Perutz, M. F. (1979) *Annu. Rev. Biochem. 48*, 327–386.

Perutz, M. F. (1980) *Proc. R. Soc. London, Ser. B 208*, 135–162.

Perutz, M. F., Heidner, E. J., Ladner, J. E., Beetlestone, J. G., Ho, C., & Slade, E. F. (1974) *Biochemistry 13*, 2186–2200.

Ribbing, W., & Ruterjans, H. (1980a) *Eur. J. Biochem. 108*, 79–87.

Ribbin, W., & Ruterjans, H. (1980b) *Eur. J. Biochem. 108*, 89–102.

Scheler, W., Schoffa, G., & Jung, F. (1957) *Biochem. Z. 329*, 232–246.

Shulman, R. G., Hopfield, J. J., & Ogawa, S. (1975) *Q. Rev. Biophys. 8*, 325–420.

Sick, H., & Gersonde, K. (1969) *Eur. J. Biochem. 7*, 273–297.

Sick, H., & Gersonde, K. (1974) *Eur. J. Biochem. 45*, 313–320.

Steffens, G., Buse, G., & Wollmer, A. (1977) *Eur. J. Biochem. 72*, 201–206.

Steigemann, W., & Weber, E. (1979) *J. Mol. Biol. 127*, 309–338.

Trittelvitz, E., Sick, H., Gersonde, K., & Ruterjans, H. (1973) *Eur. J. Biochem. 35*, 122–125.

Wüthrich, K. (1970) *Struct. Bonding (Berlin) 8*, 53–121.